land

MDPI

Article

Projecting Future Land Use Distributions to Enhance Ecosystem Service Value: A Dyna-CLUE Modeling Approach

Tianhai Zhang [1,2,*], Shouqian Sun [1,*], Zhibing Zou [1,3], Rong Zhang [1,4] and Greg Foliente [5,6]

[1] Zhejiang Key Laboratory of Intelligent Systems and Equipment for Digital Creativity, Zhejiang University, Hangzhou 310058, China
[2] Department of European Design, Sichuan Normal University, Chengdu 610101, China
[3] School of Art Design, Zhejiang Guangsha Vocational and Technical University of Construction, Jinhua 321000, China
[4] College of Landscape Architecture and Art, Fujian Agriculture and Forestry University, Fuzhou 350002, China
[5] Department of Infrastructure Engineering, The University of Melbourne, Parkville 3010, Australia; greg.foliente@unimelb.edu.au
[6] Advanced Research Institute for Informatics, Computing and Networking (AdRIC), College of Computer Studies, De La Salle University, Manila 1004, Philippines
* Correspondence: thzhang@sicnu.edu.cn (T.Z.); ssq@zju.edu.cn (S.S.)

Abstract

Land use change is the most direct factor driving the supply and alteration of ecosystem services. This study employed the Dyna-CLUE tool to simulate future land use distributions under two scenarios—the Constrained Trend (CT) and Optimized Target-driven (OT) scenarios—based on land use data from 2010. Subsequently, their corresponding ecosystem service values (ESVs) were calculated, with the simulation outcomes revealing distinct land use layouts under each scenario. Under the CT scenario, grassland and urban areas expanded, whereas farmland and water bodies declined, reflecting a trend of urbanization at the expense of rural landscapes. In contrast, the OT scenario demonstrated a cessation of built-up land expansion, accompanied by marked increases in forest and water coverage, changes that facilitated the restoration of coastal watersheds, enhancing wetland provision and improving overall ESV. Consequently, per capita ESV increased substantially—from 1751 CNY in 2018 to 2356 CNY, matching the 2010 level—primarily due to the conversion of grasslands and farmlands into forests and wetlands. The OT scenario also improved the spatial distribution of ESVs, forming interconnected ecological zones around urban areas. The results underscore that policies restraining built-up expansion, promoting afforestation, and restoring wetlands can significantly improve ecosystem services and contribute to sustainability.

Keywords: land use; ecosystem services value; Dyna-CLUE; Xiamen

Check for updates

Academic Editor: Corrado Zoppi

Received: 27 February 2026
Revised: 24 March 2026
Accepted: 27 March 2026
Published: 29 March 2026

Copyright: © 2026 by the authors. Licensee MDPI, Basel, Switzerland. This article is an open access article distributed under the terms and conditions of the Creative Commons Attribution (CC BY) license.

1. Introduction

Land use represents the most direct interface between human activities and the natural environment, encompassing multiple utilizations for various socio-economic purposes [1–3]. Land use and cover change (LUCC) plays critical roles in worldwide environmental change and serves as a major driver of alterations in terrestrial systems [4,5]. LUCC influences a wide range of natural phenomena and ecological processes, including biodiversity and surface runoff, thereby inducing shifts in ecosystem structure and function [6–8]. Consequently, land plays a foundational role in sustaining ecosystem ser-

vice functions, making LUCC a primary determinant of changes in terrestrial ecosystem services [9,10].

The widely accepted definition of ecosystem services encompasses the direct and indirect benefits that humans obtain from ecosystems; these benefits are essential for human survival, economic activity, and well-being, and include four main services—provisioning, regulating, cultural, and supporting [11,12]—which serve as core indicators for assessing a region's capacity to achieve sustainable development. Ecosystem service value (ESV) represents an evaluation approach that quantifies, in monetary terms, the direct and indirect benefits obtained from ecosystem functions [9]; the spatial pattern of ESVs is closely linked to the configuration of natural geographical features and patterns of socio-economic development [13]. Quantifying ESV facilitates a clear and intuitive understanding of spatiotemporal variations in ecosystem services, thereby offering a concrete data-driven foundation for rational land use planning and urban ecosystem optimization, ultimately supporting sustainable urban development [14,15]. In 1997, Costanza et al. pioneered the principles and methodologies for estimating ESV. Building upon Costanza's framework, Xie Gaodi and colleagues adapted the valuation system to align with China's specific ecological and socio-economic contexts, establishing a tailored ESV assessment model for Chinese ecosystems [16,17].

Currently, research on the influence of land use change on ESV has predominantly emphasized historical and contemporary assessments, while studies addressing the ecological implications of future land use changes remain relatively limited [18,19]. By validating historical and current data, forecasting future land use patterns, and estimating their associated ESVs, it is possible to develop robust technical approaches for the optimization of land use management and planning, thereby enhancing ecosystem functions and advancing sustainable urban development [20–22].

A variety of methods exist for simulating LUCC [23–25]; among these, the Conversion of Land Use and its Effects at Small Regional Extent (CLUE-S) model enables a quantitative analysis of the relationships between LUCC and its driving factors—including social, economic, technological, and environmental variables—thereby uncovering fundamental patterns of spatiotemporal land use evolution and facilitating predictions of future changes [26]. In comparison to other models, Dyna-CLUE, as the most recent version of CLUE-S, offers distinct advantages, including high accuracy in small-scale simulations, the integration of driving factors of both nature and socio-economy during the modeling process, and the capacity to spatially visualize optimization outcomes [27].

Since 2000, urbanization in China has continuously accelerated, with the urbanization rate having risen to 63.89% by 2020; this rapid urban expansion has resulted in the large-scale conversion of ecological lands, including farmland, watersheds, and grasslands, into built-up areas, thereby disrupting ecosystem structures and impairing service functions [28–30]. Consequently, assessing the land use changes and related evolution of ecosystem services during urbanization serves as a critical foundation for optimizing urban planning and enhancing ecosystem services [31,32], which is essential for advancing sustainable urban development [33,34].

In this study, the coastal city of Xiamen, China, was chosen as the study area to simulate land use change and optimize ecosystem services. Xiamen's historical connection to global trade dates back to its role as one of the five treaty ports during the late Qing Dynasty. Following China's reform and opening-up policy in 1978, Xiamen was designated as one of the initial five Special Economic Zones. Over more than four decades of rapid industrialization and urbanization, the land use structure in Xiamen has undergone substantial transformation, leading to significant alterations in ESV and intensifying the conflict between human activities and land resources [35].

A previous study focused on the spatiotemporal pattern evolution and profit–loss analysis of ESV during a historical period [36]. Building upon this foundation, this research extends the perspective toward the future, aiming to explore the "pathways to reversal" of the declining ESV trend. Consequently, this study introduces a two-dimensional comparison between "target optimization" and "real-world constraints;" specifically, one scenario is the "Constrained Trend Scenario (CT)," which adheres to real-world physical boundaries and socio-economic constraints, reflecting a cautionary picture of "where inaction will lead in the future;" the other is the "target-based regulation scenario (Optimized Target-driven scenario, OT)" based on the per capita ESV welfare target.

Therefore, this study involves setting a clear policy objective—"restoring the per capita ESV level to that of 2010"—to inversely deduce the optimal allocation path of the land system. Thus, the "per capita welfare" indicator is introduced as a regulatory benchmark. When setting ecological restoration goals, most studies use total restoration or percentage increase as standards; this research keenly captures the characteristic of Xiamen as a city with a net population inflow and proposes using "per capita ESV" as the regulatory anchor, an approach that not only considers the absolute quantity of ecological land, but also responds to the dilution effect of population growth on ecological dividends, reflecting the people-oriented philosophy of ecological civilization.

Generally, the method in this research, combining "forward simulation" with "backward tracing," enhances the goal orientation and policy relevance of scenario simulation. Furthermore, setting the target of restoring the low level of 2018 to the per capita level of 2010 is a quantitative goal that is both challenging and aligned with the demands of high-quality development, making the simulation results more practically significant for guidance.

2. Materials and Methods

2.1. ESV

2.1.1. Calculation of ESV

The evaluation of ESV was proposed by Costanza et al., and it was widely used for ecosystem service research [14]. The ESV calculation equation is as follows:

$$ESV = \sum V_i \times A_i \quad (1)$$

where ESV represents the sum value in the research area; V_i represents the per-unit-area value for land use type i; and A_i represents the total area for land use type i in the research area.

Building upon the foundational valuation methods established by Costanza et al., and grounded in the theory that individual preferences, willingness to pay, and ESV represent forms of utility value, Chinese scholars led by Xie Gaodi revised the unit price system for ecosystem service evaluation in 2007. The evaluation framework developed by Xie has been widely adopted for ESV accounting in China. Although subsequent studies have proposed refinements to this system, the majority of these adaptations remain fundamentally based on Xie's original ESV evaluation methodology [37–39].

Therefore, to account for regional specificity, and given Xiamen's location within Fujian Province, this study adopts the methodological framework established by Xie et al., utilizing ESV calculation parameters derived from Kai Su et al.'s research on Fujian Province. All the coefficients in Su's research on ESV were adjusted to local conditions by incorporating provincial data on Net Primary Productivity (NPP), the Consumer Price Index (CPI), and grain yields in Fujian Province [40] (Figure 1). While ESV coefficients may vary across spatial scales, leading to potential differences in absolute ESVs compared to those derived

from localized coefficients, the consistent use of provincial-level ESV coefficients across all periods ensures temporal comparability (1989–2030) and does not undermine the reliability of our core conclusions, especially the relative differences and spatial heterogeneity of ESV improvement based on comparison.

Primary classification	Supply service		Regulatory service				Support service		Cultural service	Total
Secondary classification	Food production	Raw material production	Gas regulation	Climate regulation	Waste disposal	Hydrological regulation	Soil conservation	Maintaining biodiversity	Provide aesthetic landscape	
Farmland	3419	1333	2461	3316	4752	2632	5025	3487	581	27,006
Forest land	1128	10,187	14,768	13,913	5880	13,982	13,743	15,418	7111	96,129
Grassland	1470	1231	5128	5333	4512	5196	7658	6393	2974	39,894
Watersheds	1812	1196	1743	7042	50,765	60,747	1402	11,726	15,178	151,612
Total	7829	13,947	24,100	29,604	65,909	82,557	27,828	37,024	25,844	
	21,776		20,2170				64,852			

Low High Equivalent coefficient

Figure 1. The specific equivalent coefficients of ESVs (components and total) for the land types in Fujian province, China [40]. Unit: Chinese yuan/ha·a.

Based on these annual flow values, changes in land use conversion and their impacts on the equivalent coefficient for per unit area value were calculated, as illustrated in Figure 2 below.

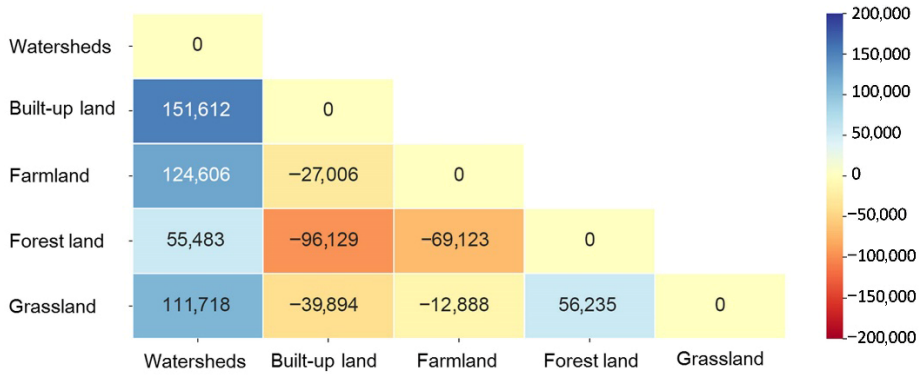

Figure 2. Changes in the equivalent coefficient due to mutual transition among land use in Fujian province. Unit: Chinese yuan/ha·a.

2.1.2. Sensitivity Analysis of ESV

Sensitivity Analysis of Value Coefficients

To test the robustness of the assessment results to the selection of value coefficients, this study employed the standard Coefficient of Sensitivity (CS) method. By adjusting the per-unit-area ESV coefficients for each land use type in Figure 1 by ±50%, the corresponding percentage changes in total ESV were calculated. The results show that the CS values for all years are substantially less than 1, indicating that the total ESV is insensitive to variations in the value coefficients. Among all land types, watersheds relatively exhibit the highest CS values, attributable to their highest per-unit-area ESV and their considerable distribution within the study area.

Sensitivity Analysis of Land Transfer Pathways

To further identify the key driving pathways responsible for ESV decline, this study conducted a transfer pathway sensitivity analysis based on the land transfer profit-and-loss matrix (Figure 2), which displays the ESV gain or loss resulting from the conversion of

one unit area between different land types, with these values derived from the differences in ESV coefficients among land use types, which are presented in Figure 2. The analysis reveals that the conversion of "forest land to built-up land" is the most sensitive loss pathway, with a unit loss of −96,129 CNY/ha, followed by the conversion of "grassland to built-up land" with a unit loss of −39,894 CNY/ha. The loss coefficients of these two pathways are substantially higher than those of other conversion types, which implies that, even if the value coefficients fluctuate within a certain range, the declining trend of ESV cannot be reversed as long as the expansion of built-up land continues to encroach upon forest land and grassland. Therefore, the core conclusion that "the expansion of built-up land is the main cause of ESV decline" exhibits strong directional robustness, and the critical leverage point for ecological regulation policies should focus on interrupting high-loss land conversion pathways.

2.2. Change History of Land Use and ESV in Xiamen

2.2.1. Study Area

Located on the southeast coast of China, Xiamen City encompasses a total study area of 1700.61 km^2. The city is bordered by the economically developed Zhejiang Province to the north and Guangdong Province to the south. Xiamen features an extensive coastline, with mountainous terrain in the north and coastal waters to the south.

Since China's reform and opening up in 1978, Xiamen has been designated as one of the initial five Special Economic Zones, undergoing rapid industrialization and urbanization. By 2020, its total population had reached five million, with an urbanization rate of 90%, significantly higher than the national average of 63.9%. In recent years, built-up land has expanded dramatically, encroaching upon ecological spaces such as farmland and watersheds. Spatially, the southern coastal areas are predominantly occupied by urban construction, resulting in fragmented and isolated patches of ecological land amidst urbanized zones. As an international tourist destination and a nationally recognized ecological garden city, Xiamen bears considerable responsibility for ecological preservation.

2.2.2. History of Land Use and ESV Change

Observation and summary of the spatiotemporal evolution of land use patterns in Xiamen City over the past three decades (1989–2018, Figure 3) reveal that built-up areas expanded continuously and rapidly throughout this period; urbanization was primarily driven by the conversion of farmland and the reclamation of coastal watersheds. Newly developed built-up land is predominantly concentrated in flat, low-lying areas along the coastline and in the immediate vicinity of existing urban centers.

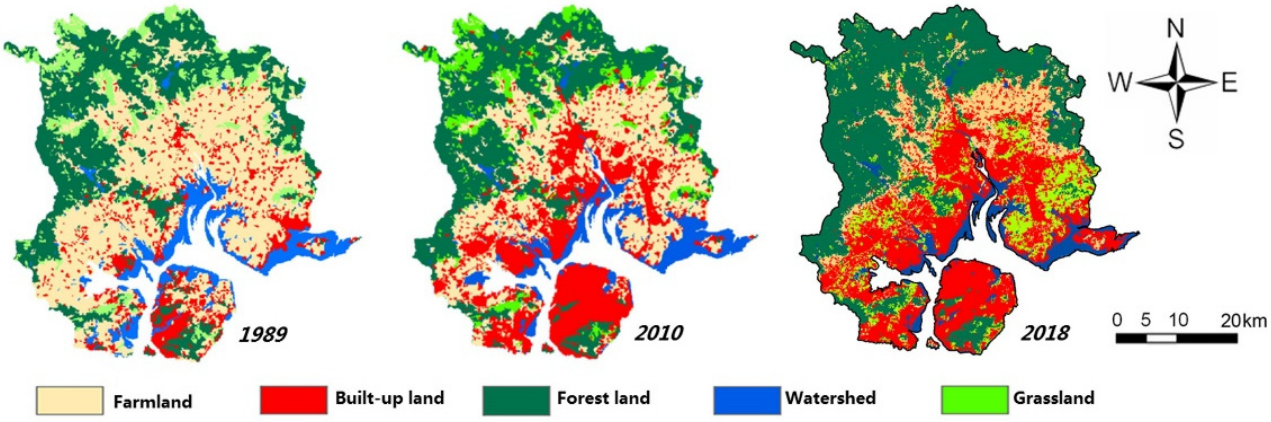

Figure 3. Spatiotemporal changes in land use in 1989, 2010, and 2018 in Xiamen city.

Meanwhile, the total ESV exhibited a continuous decline, indicating that rapid economic development and intensive urban expansion during this period resulted in a substantial loss of ecosystem services. In 1989, the per capita ESV stood at 8202.3 CNY; by 2010, however, it had decreased to 2355.5 CNY, representing only 28.7% of the 1989 level. More critically, by 2018, the per capita ESV had further declined to 1750.5 CNY, merely 21.3% of its initial value.

A detailed and in-depth analysis of historical changes in ESV from 1989 to 2018 revealed that farmland and watersheds were the primary contributors to the overall reduction during this period. The substantial decline in these land types resulted in their gradual replacement by areas with low ESV, particularly built-up land, a shift which has led to the degradation of key ecosystem services, such as water conservation and waste disposal, ultimately driving the observed downward trend in total ESV.

To advance sustainable development and support Xiamen's transition toward an eco-city, this study aims to counteract the ongoing decline in ESV and enhance it through strategic land use optimization. Considering that the reductions in farmland, grassland, and watersheds from 2010 to 2018 all exceeded those observed from 1989 to 2010, 2010 serves not only as a turning point marked by dramatic changes in the rate of land transformation, but also as an achievable target for the restoration and enhancement of per capita ESV; thus, given the negligible population growth in Xiamen since 2020 (remaining within 1%), this research takes per capita ESV at the 2010 level as the objective of restoration, under the assumption of a stable future population.

2.3. Dyna-CLUE

The Dyna-CLUE model is founded on the premise that regional land demand serves as the primary driver of land use change, maintaining dynamic equilibrium with land use distribution, natural environmental evolution, and socio-economic development. Consequently, the model structure comprises two integrated components: modules of land spatial allocation and demand. The former utilizes the non-spatial land demand projections, along with raster-based spatial data, to simulate future land use patterns based on distribution probabilities and allocation rules for each land category; the latter estimates the annual quantity of single land types in various scenarios by analyzing natural and anthropogenic factors through mathematical and economic modeling.

The input requirements for the Dyna-CLUE model include the following components:

Restricted Areas: These refer to zones within the study area where land use patterns remain unchanged, such as nature reserves, reflecting constraints imposed by spatial policies and land tenure. The data must be provided in the form of a restriction map, with a grid resolution consistent with other spatial inputs. In this study, strict ecological protection and evolutionary restrictions were imposed on terrestrial freshwater areas, such as large freshwater lakes and reservoirs, which were designated as restricted areas.

Land Use Conversion Rules and Elasticity Coefficients: These parameters define the permissible transitions between land use types and the degree of reversibility associated with each conversion.

In the final simulation, from 2010 to 2030, considering the likelihood of land transfer, the elasticity coefficients are 0.2, 0.9, 0.2, 0.9, and 0.2 according to the land type order in Figure 2. All such parameters were set in a "main.1" file, configuring the entire model run by specifying key parameters and linking all necessary input files for spatial allocation.

Land Demand Scenario File: This document specifies the projected annual total area for a single land use type over the simulation period. After each simulation, based on the land demand data for the target year (namely "demand.in1"), the model generates spatial land data for each intermediate year from the initial year to the target year, namely "age.*".

The land demand settings for this study's primary target year of 2030 are presented in the Section 3.

Correlation between spatial distribution of land use and driving factors: The Dyna-CLUE model employs logistic regression to estimate the probability of occurrence for a single land use type in every grid cell, thereby quantifying the impacts of different driving factors on spatial land use distribution.

The final coefficient results for 2010, and the related land demand in 2030 used for the future simulation, are presented in the following sections, under data and processing.

2.3.1. Scenario Descriptions

(1) Constrained Trend (CT) Scenario

Under this Scenario, future land demand in Xiamen for the year 2030 is projected via the continuation of land use change trends observed between 1989 and 2018; this simulation represents a "minimum intervention" path, growing as naturally as possible under existing conditions, with only the farmland protection baseline enforced, and it addresses a key question: How would Xiamen's land use evolve without systematic ecological optimization, and only following mandatory farmland protections?

(2) Optimized Target-driven (OT) Scenario

In contrast to the scenario based on real-world constraints, this study establishes a "reverse regulation scenario", anchored to a per capita ESV welfare target; this normative, goal-oriented scenario is specifically designed to explore potential pathways for reversing the observed decline in ESV. Thus, this scenario incorporates strict conversion constraints for forest and water areas through adjusted elasticity coefficients, while also halting further expansion of built-up land, in an approach that aims to restore ecological functionality and significantly enhance ESV.

Based on the ESV coefficient table, forest land and water bodies are identified as the most impactful land use categories contributing to ESV in Xiamen; these ecological land types play critical roles in improving regional environmental quality. Consequently, the key strategy within this scenario involves the preservation and active expansion of forest and water coverage.

In alignment with the *Special Plan for Ecological Restoration of Land Space in Xiamen*, issued by the Xiamen Natural Resources and Planning Bureau [41], which enforces stringent protection of basic farmland, the grassland areas—accounting for 92% of their 2010 extent—in this scenario are designated for conversion into forest and water zones; this targeted land use transformation is intended to substantially elevate overall ESV.

This represents a normative, target-driven scenario, rather than a predictive forecast. The selection of this target is justified by its representation of a past state with higher per capita ESV, serving as a normative benchmark for desirable improvement. It is important to clarify that the resulting land use pattern represents a feasible allocation under strong assumptions, not an optimal or most likely future.

2.3.2. Data and Processing

The data for this research primarily consist of multiple data sets, including the land use vector, digital elevation model (DEM), and road network maps for the years 1989, 2000, 2010, and 2018, as provided by the Chinese Academy of Sciences. The land use data were finally classified into five types: built-up land, forest land, watersheds, grassland, and farmland.

Extensive multi-period simulation experiments conducted in the early stages of this study show that when the resolution is increased (e.g., to 30 m), the difficulty of simulation

increases significantly with the rate of simulation errors rising rapidly. For the CLUE-S model employed in this study, finer resolution would increase spatial detail but also introduce greater parameter uncertainty that may outweigh any accuracy gains. High-resolution imagery captures fine-scale heterogeneity that can interfere with statistical modeling of macroscopic land-use drivers, whereas the selected drivers—such as DEM and slope, which are primarily topographic and locational variables—exhibit more stable gradient relationships at coarser scales. Therefore, the 100 m resolution enables more robust pixel-to-driver response relationships while minimizing model error. It balances computational efficiency with spatial detail at the regional scale, removing fine "salt-and-pepper" noise while preserving core landscape patch structure.

(1) Driving Factors

In accordance with the model user manual and taking into account data availability, this study derived several proximity-based driving factors through Euclidean distance analysis in ArcGIS 10.0, including distance to coastline (DTC), distance to district center (DTD), distance to town center (DTT), and distance to road network (DTR). Additionally, a slope raster was generated from the digital elevation model (DEM).

Xiamen's topography descends from the northwest to the southeast, characterized by low mountains and hills in the northwest and coastal plains in the southeast. As a typical coastal mountainous city, Xiamen's land use pattern is profoundly constrained by the dual pressures of topographic gradients and spatial accessibility. Areas with steep slopes typically entail greater development difficulty and higher costs, and are often delineated as ecological redline zones in planning policy. Conversely, on low-gradient coastal plains, built-up land is highly concentrated.

Furthermore, Xiamen has undergone a leapfrog development from an "island city" to a "bay city." Distance-related factors effectively capture the spatiotemporal gradient of this urban expansion. Xiamen's cropland resources are inherently scarce, with high-quality arable land primarily distributed in low-lying plains adjacent to towns (i.e., areas with small DTD and gentle slopes); driven by distance-related factors, these areas become the primary targets for built-up expansion, leading to a "spatial crowding-out" effect on high-quality farmland.

Technically, all six resulting spatial layers were output as raster maps at a consistent 100-m resolution and served as input driving factors for the model; these raster data sets were subsequently converted into ASCII format to ensure compatibility with the Dyna-CLUE modeling framework.

(2) Logistic Regression and Model Validation

Logistic regression is a nonlinear statistical method used in change studies, suitable for modeling binary dependent variables; this approach typically entails discretizing the study area into grid cells and employing stepwise logistic regression to estimate the probability occurrence for a specific land use type occurring in every single cell, based on spatial distribution of land use categories and their associated driving factors. The analysis facilitates the identification of factors that exert significant influences on land use patterns, while excluding those that are statistically insignificant.

As shown in Figure 4, for the year 2010, after the multicollinearity diagnostic with results below the accepted threshold, the logistic regression was performed with results that only 4 out of 30 cases were non-significant. Moreover, the Area Under the Curve (AUC) from the Receiver Operating Characteristic (ROC) for all regression equations across the five land types exceeded 0.8, indicating that the selected driving factors possess strong explanatory power and are suitable for regional simulation within the model.

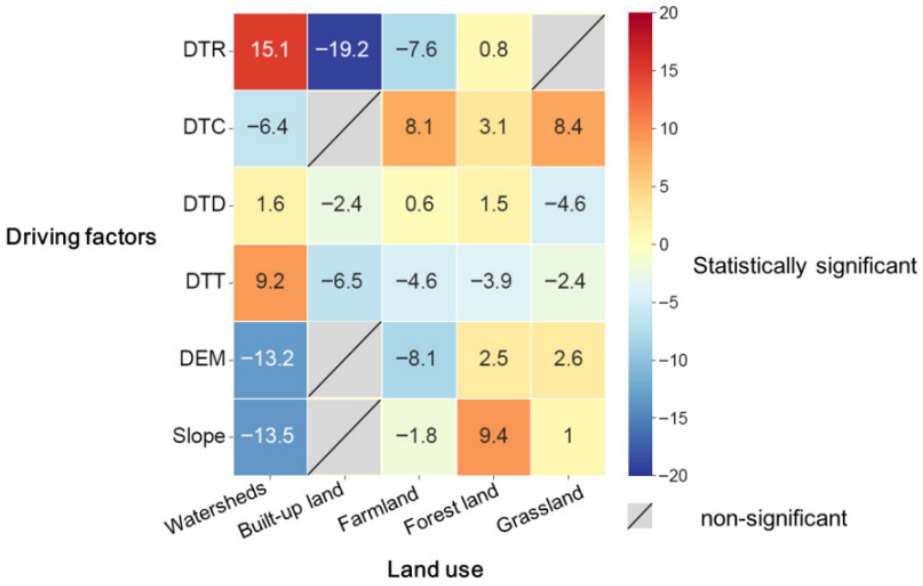

Figure 4. Coefficients of logistic regression of land use with driving factors in 2010 in Xiamen city. 'non-significant' means the *p* value is more than 0.05.

The Kappa coefficient was calculated by comparing observed land use data, derived from remote sensing, with simulated land use distribution in the same reference year. A Kappa value of no less than 0.7 is generally considered to reflect satisfactory simulation performance.

In this simulation research, for the preliminary stage, we conducted extensive simulation tests and experiments, as shown in Figure 5, below. We examined both the error matrix and the Kappa coefficient simultaneously and found that, in most cases, especially over a ten-year period, the simulation accuracy was high, with the Kappa coefficient meeting the requirement (>0.7); it can also be observed that the longer the simulation period, the lower the accuracy.

	Watershed	Built-up land	Farmland	Forest land	Grassland	Total
Actual in 2000	15,261	21,649	62,407	46,762	15,203	161,282
Correct for 1989–2000	11,412	18,030	55,606	45,309	14,969	145,326
	0.748	0.833	0.891	0.969	0.985	0.901
Actual in 2010	13,539	40,240	47,288	47,186	13,029	161,282
Correct for 1989–2010	9759	23,754	33,099	42,609	9506	118,727
	0.721	0.590	0.700	0.903	0.730	0.736
Correct for 2000–2010	9882	25,924	36,191	44,189	10,731	126,917
	0.730	0.644	0.765	0.936	0.824	0.787
Actual in 2018	10,586	49,072	17,779	57,834	26,011	161,282
Correct for 1989–2018	5986	30,962	7511	47,414	6701	98,574
	0.565	0.631	0.422	0.820	0.258	0.611
Correct for 2000–2018	6490	31,127	7675	47,523	6862	99,677
	0.613	0.634	0.432	0.822	0.264	0.618
Correct for 2010–2018	7411	33,349	7620	48,227	7824	104,431
	0.700	0.680	0.429	0.834	0.301	0.648

Actual cells | Correct cells in simulation | Simulation accuracy rate (Low — High)

Figure 5. Simulation results and accuracy matrices for different periods.

From Figure 5 above, it can be seen that, although the simulation accuracy for 1989 to 2000 on a decadal scale was high, the accuracy significantly decreased as the time span lengthened (with greater amount of land use change), and it was even lower than the accuracy of the 2010 simulation for 2018. Therefore, considering that the simulation

for 2030 covers a relatively long period, this study uses 2010 data to simulate the land distribution for 2030 (Figure 6).

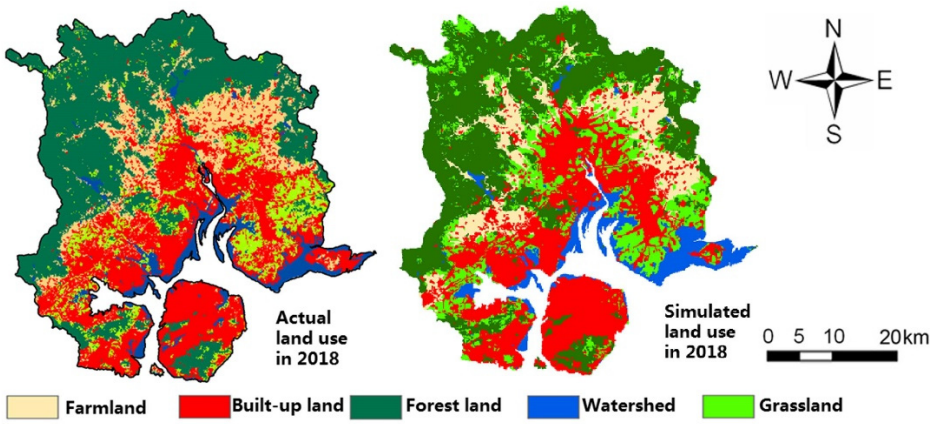

Figure 6. The actual and simulated distributions of land use in 2018 in Xiamen city.

3. Results

3.1. Land Use Demand

The final settings of area demand for each land type under different scenarios and the 2018 baseline are shown in Table 1.

Table 1. Land use areas in 2018 and under the demand settings of the two scenarios.

Scenario	Watershed	Built-Up Land	Farmland	Forest Land	Grassland	Total
2018 actual	10,586	49,072	17,779	57,834	26,011	161,282
OT in 2030	25,807	49,072	6887	78,487	1029	161,282
CT in 2030	3338	61,740	6887	57,834	31,483	161,282

Constrained Trend (CT) scenario

In this scenario, curve fitting was first applied to the historical trends (1989–2018) of single land use types to project the respective land areas in 2030 (Figure 7). Based on the optimal fitting results, built-up land exhibits a linear growth trajectory, reaching 61,740 hectares by 2030. For watersheds and farmland, the cubic function provided the best fit to historical data, projecting watershed area to reach 3338 hectares by 2030. However, the projected value for farmland, approximately –72,002 hectares, was deemed unrealistic.

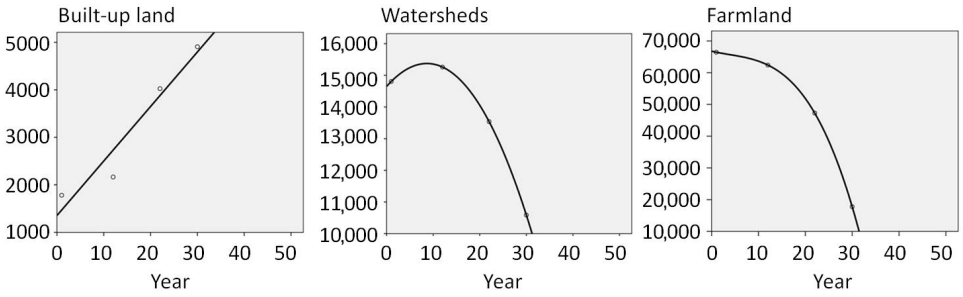

Figure 7. Observed data and curve estimation of built-up land, watersheds, and farmland in 2030.

To prevent continued reduction in farmland, the *Special Plan for Ecological Restoration of Land Space in Xiamen City* mandates strict adherence to the preservation target of 6887 hectares of permanent basic farmland [41]. Accordingly, the farmland area for 2030 was set to 6887 hectares.

Therefore, although this scenario is based on historical trends, it has undergone a necessary 'correction' because it violates the bottom line of reality. It should be understood as a scenario of 'growing as closely as possible to nature under the constraints of reality'; this "minimum intervention"-corrected natural growth scenario is designed to address a key scientific question: What trajectory would Xiamen's land use pattern follow in the absence of systematic ecological optimization measures and with only the farmland protection baseline being observed?

Given that forest land area remained stable between 1989 and 2018, the 2030 forest area was maintained at the 2018 level of 57,834 hectares. The remaining area, totaling 31,483 hectares, was allocated to grassland. Although this exceeds the 2018 grassland area, it aligns with the overall trend observed from 1989 to 2018. While the curve-fitting model projected grassland area to reach 98,165 hectares by 2030, this outcome was considered infeasible due to the non-negativity constraint of farmland. Therefore, the final grassland area was rationally adjusted to 31,483 hectares.

Optimized Target-driven (OT) scenario

The land allocation strategy under this scenario prioritizes the conservation of watersheds and forested areas, aiming to reduce their conversions to other land use types. To enhance both total and per capita ESV in Xiamen, this study proposes an expansion of forest and watershed coverage. Given the assumption of a stable population and the practical irreversibility of built-up land conversion, the extent of urban area is maintained at the 2018 level. Consequently, increases in forest and water areas must be achieved through reductions in farmland and grassland.

Farmland was set at a minimum of 6887 hectares, in compliance with existing regulatory targets, while built-up land remained unchanged at 49,072 hectares (2018 level). Grassland was allocated 1029 hectares to maintain essential urban green infrastructure. To restore per capita ESV to the 2010 benchmark of 2355.5 CNY, watershed area needed to be expanded to 25,807 hectares. The remaining land area was allocated to forest, totaling 78,487 hectares—a substantial increase from the 57,834 hectares recorded in 2018—which is expected to significantly contribute to ESV enhancement.

3.2. Change in Land Use Distribution

Following the simulations and validation, Dyna-CLUE was employed to project land use in 2030 for Xiamen. Simulations were conducted under two scenarios: a natural growth scenario with reality constraints (Constrained Trend, CT, scenario) and an ESV improvement scenario with a specific target (Optimized Target-driven, OT, scenario); these projections, which used the 2010 land use map as a baseline alongside other spatially prepared data inputs, are presented in Figure 8.

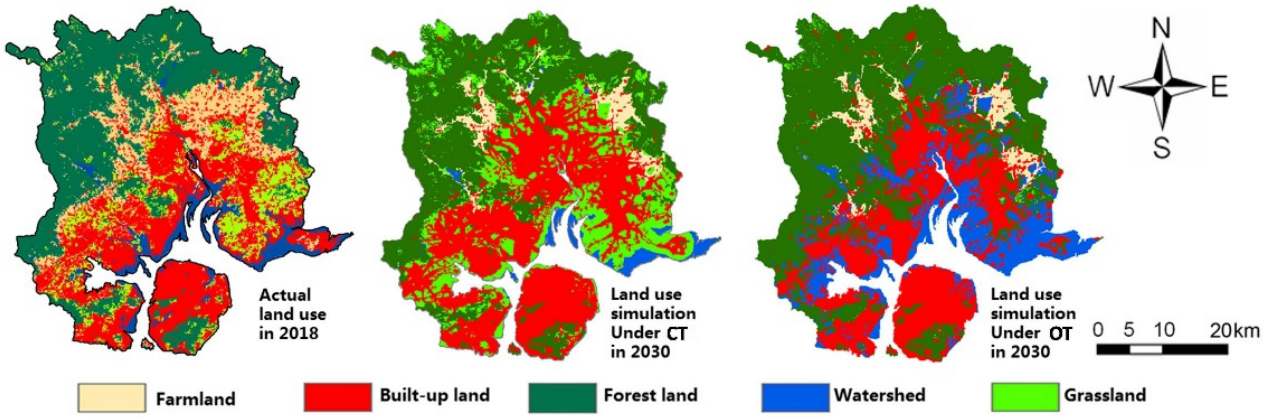

Figure 8. Simulated land use in 2030 under two scenarios and actual land use distribution in 2018.

In the CT scenario for 2030, the spatial distribution of the built-up and forest lands remains largely consistent with the 2018 baseline; in contrast, significant changes are projected for farmland, watersheds, and grassland (Figure 8).

Although farmland experienced a notable decline by 2018, it remained the predominant land cover type, distributed extensively between built-up areas and forests along a southwest–northeast corridor. The 2030 simulation, however, projects sharp reductions in both the total area and spatial extent of farmland; its distribution becomes concentrated primarily in the northwestern and northeastern sectors of the study area (Figure 8).

The above transformation is driven by the rapid expansion of built-up land. Thus, to accommodate this growth, land conversions occur primarily at the expense of watersheds, farmland, and forest land. Consequently, urban extent reaches its maximum under this scenario, with dense, patchy clusters of built-up land proliferating notably along the coastline and expanding outward from the 2018 urban core. Concurrently, grassland continues its expansion from 2018, encroaching upon vast tracts of farmland that formerly encircled the urban area (Figure 8).

These spatial patterns suggest a strong correlation between urban economic growth and rural land use change. The simulation indicates that, as the urban economy expands, surrounding populations are likely to migrate towards urban centers seeking higher incomes; this rural exodus, coupled with the proximate expansion of built-up land, appears to drive the degradation of peri-urban rural areas, ultimately leading to the abandonment of farmland and its subsequent transition to grassland.

Under the OT scenario, a marked increase is observed in the coverage of high-ESV land cover classes—watersheds and forest land—by 2030 compared to the 2018 baseline (Figure 8). Quantitatively, the area of watersheds is projected to increase from 6.6% to 16%, while forest land will expand from 36% to 49% of the total study area.

Although forest cover increases substantially, its spatial distribution remains largely unchanged, maintaining a concentrated and contiguous pattern. The distribution of grassland and farmland becomes increasingly confined to the northern mountainous regions. Characterized by high elevation and significant distance from existing built-up areas and coastlines, this zone represents the core area of forest aggregation (Figure 8). Conversely, both farmland and grassland undergo significant reductions in their overall scale and spatial extent. Land in elevated areas primarily undergoes conversion to forest, while lower-lying areas are transformed into coastal water bodies and wetlands.

Due to the implementation of protected zoning, farmland remains stable in contiguous blocks within the northeastern and northwestern sectors. However, in mountainous terrain and on higher ground proximal to urban areas, farmland is gradually abandoned and reverts to forest land, a transition attributed to a combination of factors, including marginal soil or water conditions and the out-migration of residents.

This scenario prioritizes the high-quality development of the urban ecological environment through targeted interventions such as afforestation, the conversion of farmland to wetlands, and artificial water replenishment. Consequently, the extent of forest land and watersheds is maintained at a significantly higher level relative to other modeled scenarios.

3.3. Change in Spatial Distribution of ESV

3.3.1. Total ESV

The spatiotemporal pattern of ESV within Xiamen for the year 2030 reveals distinct patterns under the natural growth scenario. High-value zones (exceeding 30 billion CNY) remain relatively stable. In contrast, medium-value zones (10–30 billion CNY) undergo a notable contraction, while low-value zones (below 10 billion CNY) experience significant spatial expansion (Figure 9).

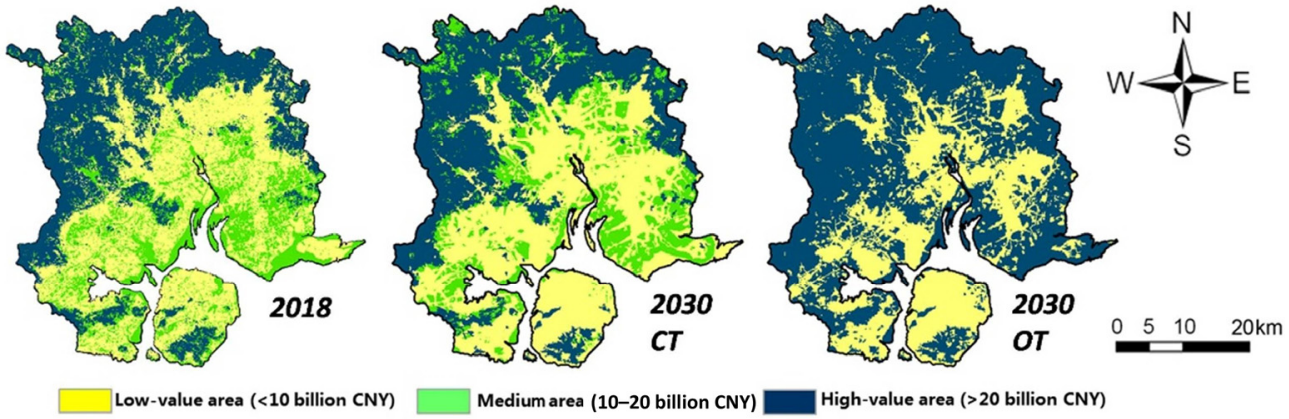

Figure 9. The ESV spatial distribution in 2018 and simulated 2030 distributions under two scenarios.

This redistribution is primarily driven by land use conversion. The decline in median-value areas is attributable to the transformation of high-value land cover types, particularly watersheds, into land cover areas with lower ESV coefficients, such as grasslands, in a process that creates a "double decline effect," whereby the loss in spatial area is compounded by a reduction in the per-unit value coefficient of the land.

Concurrently, the expansion of low-value areas results from two synergistic factors: the direct increase in the spatial extent of built-up land (which possesses a very low ESV coefficient) and the concomitant decrease in the area of high-coefficient watersheds.

Under the OT scenario, the spatial pattern of ESV in 2030 is characterized by a pronounced polarization (Figure 9). High-value and low-value areas both exhibit significant expansion, whereas the medium-value zone undergoes a substantial contraction.

The enlargement of high-value areas is predominantly attributed to the increased areal extent of high-coefficient land cover types, specifically forest land and watersheds; this scenario facilitates the ecological enhancement of grasslands, the majority of which are successfully converted into these higher-value land classes (forests and watersheds), with minimal conversion to lower-coefficient land types, such as farmland or built-up land.

Concurrently, the process of urbanization drives the rapid proliferation of extremely low-ESV zones, which form concentric patterns around urban cores and exhibit a linear distribution along major transportation corridors, such as railway lines. In contrast, the expansion of high-value areas is primarily concentrated in coastal regions and topographical lowlands.

3.3.2. ESV Components

The spatial distribution of ecosystem services under the CT scenario remains largely consistent with the 2018 baseline, showing no significant variation across its constituent components. In stark contrast, the OT scenario reveals substantial spatial reorganization.

Within this proactive conservation scenario, the high-value areas for cultural (CS), regulating (RS), and provisioning services (PS) exhibit notable increases in their areal extents relative to both the 2018 baseline and the CT projection (Figure 10). Furthermore, the spatial distribution of these high-value zones undergoes significant expansion, extending beyond their original concentration in the northern high-elevation mountains into topographical lowlands and coastal regions.

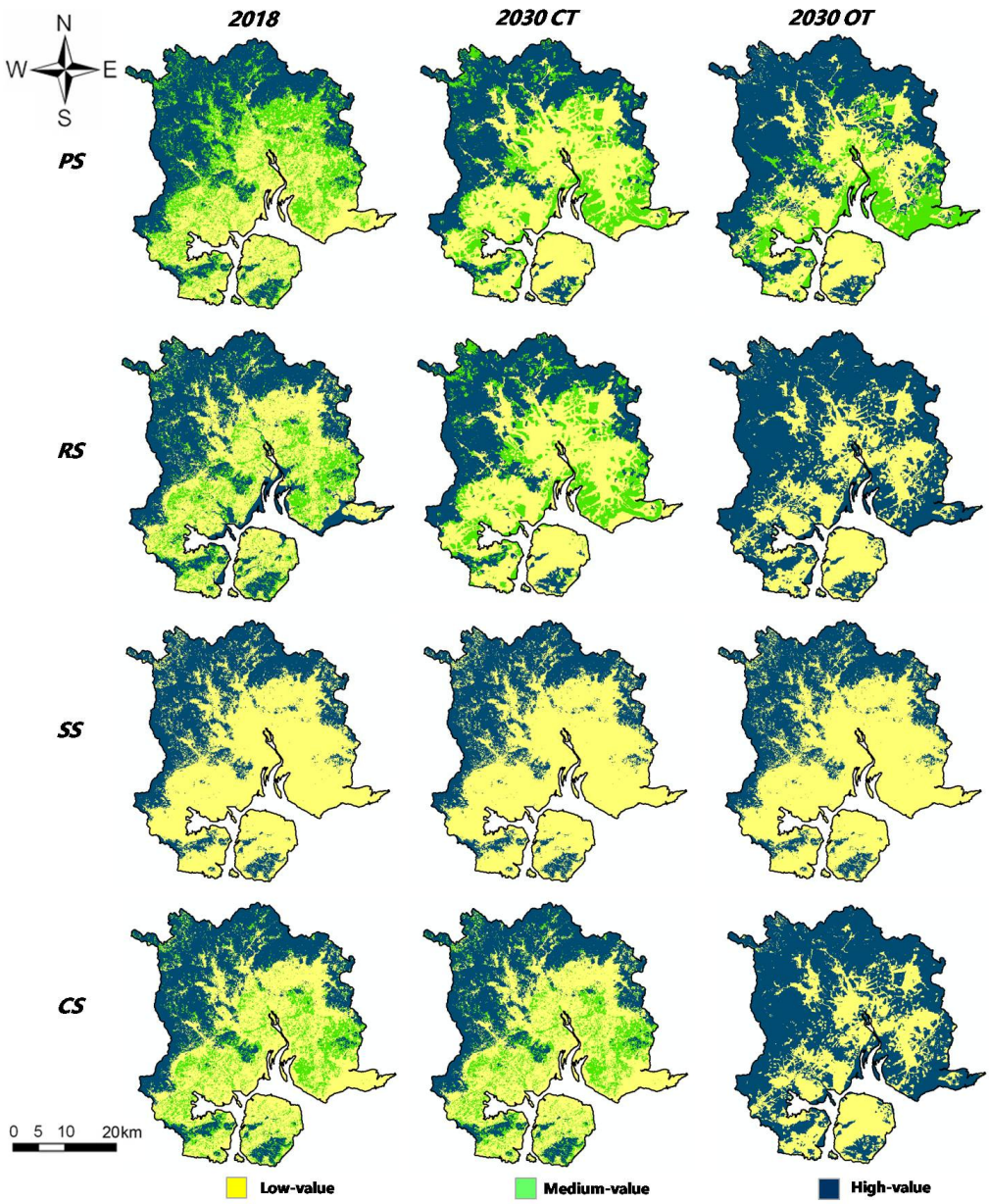

Figure 10. The spatial pattern of the ESV components in 2018 and simulated patterns in 2030 under two scenarios.

Under the OT scenario, median-value zones for cultural (CS), regulating (RS), and provisioning services (PS) are entirely eliminated, primarily as a consequence of the extensive conversion of grasslands—which previously constituted these median-value areas—into land cover types associated with higher ESVs, namely watersheds and forests.

Furthermore, the spatial distribution of medium-value areas for provisioning services (PS) under the OT scenario diverges markedly from the patterns observed in both the 2018 baseline and the natural growth scenario. Historically, these median-value PS areas were predominantly located in inland mountainous regions, characterized by grassland coverage (Figure 10). Conversely, in the OT scenario, the median-value areas for PS are largely confined to the coastal zone, primarily composed of watersheds.

Under the OT scenario, the spatial configuration and composition of low-value areas exhibit minimal divergence from the 2018 baseline and the CT scenario; this consistency arises because these zones predominantly comprise built-up land and farmland, land cover types whose distribution remained largely unchanged across all three contexts.

In summary, Xiamen's extensive coastline confers significant benefits to the regional ecological environment, enhancing key functions such as climate regulation, hydrological modulation, waste treatment, and the provision of aesthetic landscapes. Conversely, urban expansion and socio-economic development have encroached upon substantial tracts of farmland and resulted in the reclamation of watersheds, processes which have exerted adverse effects on multiple dimensions of watershed ecosystem services, culminating in a net decline in overall ecosystem functionality. The land use simulations for the OT scenario demonstrate that targeted planning interventions can facilitate the restoration of coastal watersheds, yielding an expanded area of high-value aquatic and wetland ecosystems, thereby significantly augmenting the total ESV within the study area.

3.4. Spatial Distribution of ESV Gain and Loss

Raster calculation within ArcGIS was employed to quantify changes in ESV per grid cell between the 2018 baseline and the two simulated 2030 scenarios. Based on the calculated differential, areas were categorized into three distinct zones: value loss zones (where ESV decreased), value gain zones (where ESV increased), and value preservation zones (where ESV remained unchanged) (Figure 11).

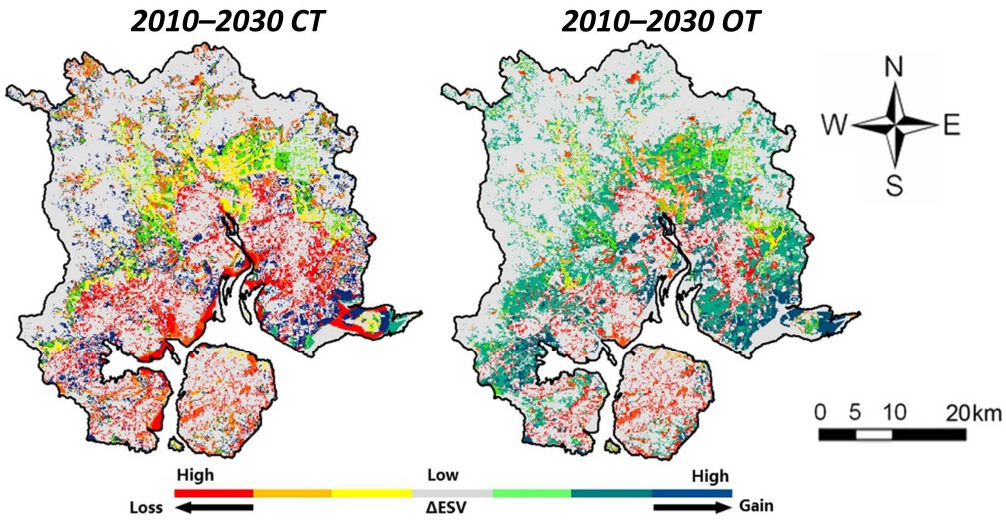

Figure 11. The spatial distributions of ESV gain and loss as simulated for 2030 under two scenarios.

As illustrated in Figure 9, value preservation zones constitute the largest proportion of the study area under both the CT and OT scenarios, accounting for 57.7% and 62.1% of the total area in the respective scenarios. Spatially, they are predominantly concentrated in the northern mountainous regions, and this distribution pattern is largely attributable to the simulated stability of built-up and forest land cover types in these areas, which exhibited minimal change in both their total extent and spatial configuration from the 2018 baseline.

Across both scenarios, value loss zones are predominantly concentrated adjacent to the 2018 built-up areas (Figure 11); however, their scale and distribution differ markedly. Under the CT scenario, these zones cover a substantially larger area (36,662 ha, 22.8%) and exhibit a more extensive spatial distribution, particularly in coastal regions, compared to the OT scenario (18,126 ha, 11.3%), a pattern consistent with the effects of rapid urban expansion, wherein substantial tracts of coastal watersheds, farmland, and grassland encircling existing urban areas have been converted.

Conversely, the scale and spatial configuration of value gain zones also diverge significantly between the two scenarios; in the CT scenario, these zones are fragmented and dispersed (Figure 11); in contrast, under the OT scenario, value gain zones form contiguous tracts concentrated around the 2018 urban periphery. The above findings stand in opposi-

tion to the historical trend observed from 1989 to 2018, wherein a significant decline in ESV was driven by the conversion of coastal farmland and watersheds to built-up land [42].

Within the OT scenario, the emergence of value gain zones is principally attributed to the strategic conversion of grasslands and farmlands into forests and watersheds. Such land use transitions can be effectively facilitated by policy instruments such as the "Grain for Green" and "Grassland to Wetland" programs. The resultant gain zones are strategically distributed around existing urban footprints and coastal areas, thereby creating a buffer that curbs urban sprawl, a configuration that fosters an integrated landscape matrix of high-ESV spaces around urban cores, rather than isolated patches. Consequently, the OT scenario not only augments the total quantum of ecosystem service value, but also optimizes its spatial distribution, promoting a more sustainable and resilient regional landscape.

4. Discussion

4.1. ESV and Food Security

The spatial distribution of simulated land use in the two scenarios exhibits pronounced divergence. The CT scenario largely perpetuates historical development trajectories, whereas the OT scenario represents a substantial departure from this trend; this divergence invites critical inquiry: Does such a deviation represent a plausible alternative, or merely an unrealistic abstraction? More specifically, could the implementation of an ESV-oriented strategy yield tangible benefits for Xiamen's transformation into an eco-city? Moreover, does this scenario prefigure a reconfigured urban form that is meaningfully distinct from that of 2018?

Both the 2018 baseline and the CT scenario reflect urban–rural polarization and socio-spatial imbalance [43,44], but the OT scenario significantly enhances ecological benefits via targeted intervention [23,24]. However, it is also necessary to carefully weigh the potential costs associated with this transformation; it should involve a trade-off between the loss of provisioning services (particularly food security) and the gains in regulating services [45,46]. The enhancement of ESV would lead to a reduction in farmland, potentially compromising local food provisioning capacity. As a highly urbanized coastal city, Xiamen already exhibits a high degree of external dependence for its food supply; further loss of agricultural space would exacerbate food security risks.

Therefore, in the process of advancing eco-city construction, a balance with multiple potential strategies must be sought between enhancing ecosystem service value and ensuring food security [47,48]. First, spatial reallocation involves relocating scattered, low-yield farmland within ecological red lines through off-site compensation while consolidating high-quality cropland elsewhere—achieving both ecological gains and stable food production. Second, multifunctional land use adopts integrated models such as paddy wetlands, agroforestry, or agritourism in areas where ecological and agricultural functions overlap, allowing a single parcel to deliver both regulating services and agricultural output. Third, intensification on retained farmland promotes precision irrigation, soil enhancement, and high-efficiency cropping techniques to increase per-unit yield, offsetting any localized cropland reduction. Fourth, zoning with flexibility distinguishes between strictly protected prime farmland and areas where gradual ecological restoration is permitted, applying context-specific management based on land suitability and ecological sensitivity.

4.2. Implications for Landscape Planning

The OT scenario facilitates diversity and balance in land composition, alleviating typical urban environmental challenges [22,49]. Meanwhile, landscape fragmentation imposes constraints on the actual delivery of ecosystem services.

Research results illustrate the differences in landscape patterns between the two scenarios. Within the context of a highly urbanized coastal city, these ecological patches are often fragmented and surrounded by built-up areas, forming isolated ecological islands. Such landscape fragmentation severely limits the actual functioning of ecological processes, as fragmented forest patches struggle to support biodiversity maintenance, and wetlands surrounded by urbanization demonstrate compromised effectiveness in water purification and flood regulation [24].

The above observations imply that attention should be paid not only to increasing the quantity of ecological land, but also to ensuring its spatial connectivity and integrity [50]. While the resolution of 100 m grid in this study strikes a balance between regional-scale analysis and computational efficiency, it is important to acknowledge its limitations in capturing highly fragmented landscapes. Specifically, the 100 m grid struggles to precisely capture small patches—such as isolated woodlands and small wetlands—and their marginal contributions to local ESV, as well as smooth the continuity and width variations of linear corridors like hedgerows and riparian zones, thereby underestimating their connectivity functions at fine scales.

Therefore, for the analysis of fine-scale ecological processes in fragmented landscapes and for future land planning and management (like constructing ecological corridors and networks for enhancing the functional integration of ecosystems), subsequent studies should integrate higher-resolution remote sensing data [9,47]. From the perspective of polycrisis theory, this is a complex project involving broader interacting pressures, such as urban expansion, wetland loss, farmland protection, ecological restoration, and corresponding climate risks, food security issues, coastal vulnerability, governance constraints, and socio-economic instability [51–53].

4.3. Limitations

Parameter settings

In the OT scenario, this research assumes an idealized situation, including no growth of built-up land and a high conversion rate of grassland. It should be noted that such settings, which underlie this experimental exploration, do not align with the developmental reality of Xiamen. The rationale for designing the scenario in this manner was to explore an idealized theoretical upper limit or maximum potential benchmark for enhancing ESV under the most stringent land use policies; this "idealized" setting is then compared with more realistic scenarios to observe and quantify the maximum ESV gap, with the aim of yielding insights that can serve as references for the trade-offs between urban development and ecological protection.

Meanwhile, when estimating the demand for farmland, the projected area yielded a negative value that was inherently unrealistic. Based on the "farmland red line" (permanent basic farmland protection) policy from Xiamen's planning documents (*Special Plan for Ecological Restoration of Land Space in Xiamen*), we adjusted the farmland demand. While this setting enhances the realism of the simulations through policy-based corrections, it may also introduce a degree of rigidity, potentially underestimating the flexibility of land use transitions in response to socio-economic pressures. Furthermore, a reduction in farmland would inevitably exert a certain degree of pressure and pose a threat to the quantity of farmland and the related food security.

Benefit transfer-style ESV coefficients

ESV coefficients may vary across spatial scales. The benefit transfer method adopted in this study references the locally adjusted ESV coefficients for Fujian Province (where Xiamen City is located). This choice was motivated by the following considerations: first, data availability—localized ESV coefficients for Xiamen City are not currently available in

the literature and the local adjustment needs multiple datasets and calculations; second, but most importantly, the objective of this study—to simulate the spatial distribution of land use to achieve the goal of enhancing ESV by 2030—focuses primarily on the relative differences and spatial heterogeneity of ESV improvement based on comparison, rather than on the precise estimation of absolute ESVs. Given this research focus, using provincial-level ESV coefficients consistently across all periods ensures temporal comparability (1989–2030). Although the absolute ESVs may differ from those derived from localized coefficients, this approach does not compromise the reliability of our core conclusions.

However, when applying such coefficients to local-level land use planning decisions, several methodological limitations warrant consideration.

The transfer profit-and-loss matrix in this study assumes that the ecological impacts of land conversion are linear. In ecological reality, however, ecosystem services often exhibit threshold effects. When the area of a critical ecological patch falls below a certain threshold, it may trigger a sharp decline in service functions, such as habitat fragmentation, leading to biodiversity loss. Such nonlinear abrupt changes cannot be captured by linearly aggregated ESV coefficients; consequently, assessments based on average coefficients may underestimate the conservation value of critical ecological nodes.

Despite these limitations, this study adopted the following measures to ensure the directional robustness of the conclusions when applying this method. First, sensitivity analysis verified the low sensitivity of total ESV changes to coefficient selection (CS < 1), demonstrating that the trend conclusion of "declining total ESV" is reliable. Second, the analytical focus was placed on relative comparisons, rather than absolute values—that is, using the transfer matrix to identify "which conversion pathways incur relatively higher losses".

For future research aiming to integrate ESV into specific land use planning decisions in Xiamen, introducing the concept of ecosystem service flows (ES flows) could be considered as it would help identify the actual spatial pathways of ecosystem services from supply areas to beneficiary areas, enabling a more precise assessment of the actual impacts of land conversion on resident welfare.

5. Conclusions

Based on land use data from 2010, this study employed the Dyna-CLUE model to simulate land use distribution under two contrasting scenarios—the Constrained Trend (CT) and Optimized Target-driven (OT) scenarios—for the coastal city of Xiamen. The model was calibrated and validated to project spatially explicit land use patterns conducive to regional sustainable development. It should be noted that this study remains a simulation of land use patterns with parameter settings under specific targets. Realizing the projected ecological benefits necessitates concrete policy interventions and planning measures, especially the balance of multiple objectives, such as food security.

In OT scenario, High-ESV zones expanded beyond their traditional concentration in the northern mountainous areas into low-lying coastal regions, forming a mosaic-like ecological matrix interspersed with developed land. This finding proposes spatial planning recommendations for the coastal city Xiamen like the following.

First, establish a "containment-embedded" ecological security pattern. At the urban fringe, leverage the northern mountains and coastal wetlands to create continuous ecological barriers that restrain urban sprawl. Within built-up areas, retain or restore scattered woodlands and water corridors as high-ESV patches embedded in the urban fabric, enhancing ecosystem service provision inside the city.

Second, adopt differentiated land use control strategies. In the northern high-elevation mountains, prioritize forest quality improvement and water conservation functions. In

low-lying coastal plains and urban-rural transition zones, focus on aquatic ecosystem restoration and wetland network construction to connect fragmented ecological spaces and enhance landscape connectivity.

Third, develop mechanisms for compatible spatial arrangements between ecological and built-up land. Within new urban development boundaries, reserve ecological corridors and blue-green spaces to promote a clustered urban form and prevent continuous sprawl. In urban renewal and infill development, encourage micro-interventions such as pocket parks and riparian greenways to increase the density and accessibility of high-ESV patches.

These recommendations aim to translate results into actionable spatial planning strategies, offering a practical pathway for achieving synergies between ecological protection and urban development in high-density coastal cities.

Author Contributions: T.Z. was responsible for the conceptualization, methodology, and writing—original draft preparation; S.S. and G.F. were responsible for the conceptualization, writing—review and editing; Z.Z. and R.Z. assisted with some of the visualization work; T.Z. and S.S. were responsible for the funding acquisition. All authors have read and agreed to the published version of the manuscript.

Funding: This work was supported by the Research Fund on Several Major Issues Concerning Enhancing the Security of Emerging Service Industry Systems, Zhejiang University (Grant number 2025-PP-11-09) and the Teaching Reform Project of Sichuan Normal University (Grant number JWC20250304).

Data Availability Statement: The original contributions presented in this study are included in the article. Further inquiries can be directed to the corresponding authors.

Acknowledgments: The first author extends his thanks to Lina Tang at the Chinese Academy of Sciences for research support and help with obtaining materials for the research. All authors extend their thanks to the editors and anonymous reviewers for their careful work and comments, which substantially helped improve this paper.

Conflicts of Interest: The authors declare no conflicts of interest.

References

1. Li, L.; Huang, X.; Wu, D.; Yang, H. Construction of ecological security pattern adapting to future land use change in Pearl River Delta, China. *Appl. Geogr.* **2023**, *154*, 102946. [CrossRef]
2. Liu, Y. Introduction to land use and rural sustainability in China. *Land Use Policy* **2018**, *74*, 1–4. [CrossRef]
3. Feng, X.; Li, Y.; Wang, X.; Yang, J.; Yu, E.; Wang, S.; Wu, N.; Xiao, F. Impacts of land use transitions on ecosystem services: A research framework coupled with structure, function, and dynamics. *Sci. Total Environ.* **2023**, *901*, 166366. [CrossRef]
4. Davison, C.W.; Rahbek, C.; Morueta-Holme, N. Land-use change and biodiversity: Challenges for assembling evidence on the greatest threat to nature. *Glob. Change Biol.* **2021**, *27*, 5414–5429. [CrossRef]
5. Feng, Z.; Sun, L. Response of spatial and temporal variations of ecosystem service value to land use/land cover transformation in the upper basin of Miyun Reservoir. *Ecol. Ind.* **2024**, *160*, 111819. [CrossRef]
6. Franco, A.L.C.; Cherubin, M.R.; Cerri, C.E.P.; Six, J.; Wall, D.H.; Cerri, C.C. Linking soil engineers, structural stability, and organic matter allocation to unravel soil carbon responses to land-use change. *Soil Biol. Biochem.* **2020**, *150*, 107998. [CrossRef]
7. Hansen, A.J.; DeFries, R.S.; Turner, W. Land Use Change and Biodiversity. In *Land Change Science: Observing, Monitoring and Understanding Trajectories of Change on the Earth's Surface*; Gutman, G., Janetos, A.C., Justice, C.O., Moran, E.F., Mustard, J.F., Rindfuss, R.R., Skole, D., Turner, B.L., Cochrane, M.A., Eds.; Springer: Dordrecht, The Netherlands, 2004; pp. 277–299.
8. Jing, X.D.; Tian, G.L.; He, Y.C.; Wang, M.R. Spatial and temporal differentiation and coupling analysis of land use change and ecosystem service value in Jiangsu Province. *Ecol. Ind.* **2024**, *163*, 112076. [CrossRef]
9. Rao, Y.; Zhou, M.; Ou, G.; Dai, D.; Zhang, L.; Zhang, Z.; Nie, X.; Yang, C. Integrating ecosystem services value for sustainable land-use management in semi-arid region. *J. Clean. Prod.* **2018**, *186*, 662–672. [CrossRef]
10. Duan, X.Y.; Chen, Y.; Wang, L.Q.; Zheng, G.D.; Liang, T. The impact of land use and land cover changes on the landscape pattern and ecosystem service value in Sanjiangyuan region of the Qinghai-Tibet Plateau. *J. Environ. Manag.* **2023**, *325*, 116539. [CrossRef] [PubMed]
11. Daily, G.C. *Nature's Services*; Island Press: Washington, DC, USA, 1997. [CrossRef]

12. Costanza, R.; D'Arge, R.; De Groot, R.; Farber, S.; Grasso, M.; Hannon, B.; Limburg, K.; Naeem, S.; O'Neill, R.V.; Paruelo, J.; et al. The value of the world's ecosystem services and natural capital. *Nature* **1997**, *387*, 253–260. [CrossRef]
13. Board, M.A. *Millennium Ecosystem Assessment*; Board, New Island: Washington, DC, USA, 2005.
14. Costanza, R.; Groot, R.D.; Braat, L.; Kubiszewski, I.; Grasso, M. Twenty years of ecosystem services: How far have we come and how far do we still need to go? *Ecosyst. Serv.* **2017**, *28*, 1–16. [CrossRef]
15. Zeng, Q.; Ye, X.; Cao, Y.; Chuai, X.; Xu, H. Impact of expanded built-up land on ecosystem service value by considering regional interactions. *Ecol. Indic.* **2023**, *153*, 110397. [CrossRef]
16. De Groot, R.; Brander, L.; Van Der Ploeg, S.; Costanza, R.; Bernard, F.; Braat, L.; Christie, M.; Crossman, N.; Ghermandi, A.; Hein, L. Global estimates of the value of ecosystems and their services in monetary units. *Ecosyst. Serv.* **2012**, *1*, 50–61. [CrossRef]
17. Xie, G.; Zhang, C.; Zhen, L.; Zhang, L. Dynamic changes in the value of China's ecosystem services. *Ecosyst. Serv.* **2017**, *26*, 146–154. [CrossRef]
18. Xie, G.; Zhen, L.; Lu, C.; Xiao, Y.; Chen, C. Expert knowledge based valuation method of ecosystem services in China. *J. Nat. Resour.* **2008**, *23*, 911–919. [CrossRef]
19. Zhao, Y.; Wang, M.; Lan, T.; Xu, Z.; Wu, J.; Liu, Q.; Peng, J. Distinguishing the effects of land use policies on ecosystem services and their trade-offs based on multi- scenario simulations. *Appl. Geogr.* **2023**, *151*, 102864. [CrossRef]
20. Buyantuyev, A.; Wu, J. Urbanization alters spatiotemporal patterns of ecosystem primary production: A case study of the Phoenix metropolitan region, USA. *J. Arid. Environ.* **2009**, *73*, 512–520. [CrossRef]
21. Vidal-Legaz, B.; Martínez-Fernández, J.; Picón, A.S.; Pugnaire, F.I. Trade-offs between maintenance of ecosystem services and socio-economic development in rural mountainous communities in southern Spain: A dynamic simulation approach. *J. Environ. Manag.* **2013**, *131*, 280–297. [CrossRef]
22. Jiang, L.; Wang, Z.; Zuo, Q.; Du, H. Simulating the impact of land use change on ecosystem services in agricultural production areas with multiple scenarios considering ecosystem service richness. *J. Clean. Prod.* **2023**, *397*, 136485. [CrossRef]
23. Lin, Z.; Peng, S.; Ding, X.; Ma, D.; Zhang, R.; Lyu, M.; Shi, S.; Niu, F.; Pan, X. Unveiling ecosystem service dynamics under land use/cover changes in a plateau lake basin: A trajectory-scenario coupled approach. *Ecol. Indic.* **2025**, *178*, 15. [CrossRef]
24. Wei, L.Y.; Mao, M.J.; Zhao, Y.X.; Wu, G.H.; Wang, H.B.; Li, M.H.; Liu, T.D.; Wei, Y.H.; Huang, S.R.; Huang, L.Y.; et al. Spatio-temporal characteristics and multi-scenario simulation analysis of ecosystem service value in coastal wetland: A case study of the coastal zone of Hainan Island China. *J. Environ. Manag.* **2024**, *368*, 122199. [CrossRef]
25. Zhou, X.; Ji, G.H.; Wang, F.; Ji, X. Identification and simulation of ecological zoning in the Yangtze River Delta (YRD) urban agglomeration based on Ecological Service Value (ESV)- Landscape Ecological Risk (LER). *J. Clean. Prod.* **2025**, *516*, 145778. [CrossRef]
26. Peltonen-Sainio, P.; Jauhiainen, L.; Laurila, H.; Sorvali, J.; Honkavaara, E.; Wittke, S.; Karjalainen, M.; Puttonen, E. Land use optimization tool for sustainable intensification of high-latitude agricultural systems. *Land Use Policy* **2019**, *88*, 104104. [CrossRef]
27. Verburg, P.H.; Soepboer, W.; Veldkamp, A.; Limpiada, R.; Espaldon, V.; Mastura, S.S.A. Modeling the spatial dynamics of regional land use: The CLUE-S model. *Environ. Manag.* **2002**, *30*, 391–405. [CrossRef]
28. Huang, D.; Huang, J.; Liu, T. Delimiting urban growth boundaries using the CLUE- S model with village administrative boundaries. *Land Use Policy* **2019**, *82*, 422–435. [CrossRef]
29. Li, X.; Tian, Y.; Gao, T.; Jin, L.; Li, S.; Zhao, D.; Zheng, X.; Yu, L.; Zhu, J. Trade-Offs analysis of ecosystem services for the grain for Green program: Informing reforestation decisions in a mountainous headwater region, northeast China. *Sustainability* **2020**, *12*, 4762. [CrossRef]
30. Cui, H.; Smith, J.; Zhang, J.; Men, W.; Li, H. Simulation of soil carbon changes due to land use change in urban areas in China. *Front. Environ. Sci. Eng.* **2013**, *7*, 12. [CrossRef]
31. Wang, J.S.; Gao, D.D.; Shi, W.; Du, J.Y.; Huang, Z.; Liu, B.Y. Spatiotemporal changes in ecosystem service value: Evidence from the economic development of urbanized regions. *Technol. Forecast. Soc.* **2023**, *193*, 122626. [CrossRef]
32. Xiao, J.; Zhang, Y.; Xu, H. Response of ecosystem service values to land use change, 2002–2021. *Ecol. Ind.* **2024**, *160*, 16. [CrossRef]
33. Zheng, H.; Li, H. Spatial–temporal evolution characteristics of land use and habitat quality in Shandong province, China. *Sci. Rep.* **2022**, *12*, 15422. [CrossRef]
34. Li, W.J.; Kang, J.W.; Wang, Y. Identifying the impacts of landscape structure on ecosystem services trade-offs among ecosystem services bundles in the Mountains of southwest China. *Ecol. Eng.* **2024**, *209*, 107419. [CrossRef]
35. Zhao, J. *Towards Sustainable Cities in China, Analysis and Assessment of Some Chinese Cities in 2008*; Springer: New York, NY, USA, 2011.
36. Zhang, T.; Qu, Y.; Liu, Y.; Yan, G.; Foliente, G. Spatiotemporal Response of Ecosystem Service Values to Land Use Change in Xiamen, China. *Sustainability* **2022**, *14*, 12532. [CrossRef]
37. Zhao, Y.F.; Zhang, X.W.; Wu, Q.R.; Huang, J.L.; Ling, F.; Wang, L.H. Characteristics of spatial and temporal changes in ecosystem service value and threshold effect in Henan along the yellow river, China. *Ecol. Indic.* **2024**, *166*, 112531. [CrossRef]

38. Song, P.H.; Yang, Q.; Wu, W.Y.; Su, T.Y.; Jiang, Y.M.; Lu, J.L.; Sun, Z.Y.; Zhang, J.; Yu, R.; Wang, P.; et al. Assessing and predicting the value of ecosystem services in Sanya city, Hainan island, China. *Ecol. Indic.* **2025**, *170*, 112967. [CrossRef]
39. Tao, Q.; Gao, G.H.; Xi, H.H.; Wang, F.; Cheng, X.B.; Ou, W.X.; Tao, Y. An integrated evaluation framework for multiscale ecological protection and restoration based on multi-scenario trade-offs of ecosystem services: Case study of Nanjing city, China. *Ecol. Indic.* **2022**, *140*, 108962. [CrossRef]
40. Su, K.; Wei, D.Z.; Lin, W.X. Evaluation of ecosystem services value and its implications for policy making in China—A case study of Fujian province. *Ecol. Indic.* **2020**, *108*, 105752. [CrossRef]
41. Xiamen Natural Resources and Planning Bureau. Special Plan for Ecological Restoration of Land Space in Xiamen City. 2021. Available online: http://zygh.xm.gov.cn/zfxxgk/zfxxgkml/zhxx/tzgg/202110/P020211014425236893034.pdf (accessed on 6 June 2025).
42. López, E.; Bocco, G.; Mendoza, M.; Duhau, E. Predicting land-cover and land-use change in the urban fringe: A case in Morelia city, Mexico. *Landsc. Urban Plan.* **2001**, *55*, 271–285. [CrossRef]
43. Chu, J.; Hu, T.; Ye, Z.; Lin, J. Progress review on land science research in 2019 and prospects for 2020: The sub-report on land resources, land use and spatial planning. *China Land Sci.* **2020**, *34*, 84–92. [CrossRef]
44. Verburg, P.H.; Tabeau, A.; Hatna, E. Assessing spatial uncertainties of land allocation using a scenario approach and sensitivity analysis: A study for land use in Europe. *J. Environ. Manag.* **2013**, *127*, S132–S144. [CrossRef]
45. Chen, D.; Wang, Y.; Bao, H. Sharing or sparing? The trade-offs among urban services, food production and ecosystem services. *Habitat Int.* **2024**, *147*, 103037. [CrossRef]
46. Peng, J.; Wang, X.; Zheng, H.; Xu, Z. Applying production-possibility frontier based ecosystem services trade-off to identify optimal scenarios of Grain-for-Green Program. *Landsc. Urban Plan.* **2024**, *242*, 104956. [CrossRef]
47. Qiu, Z.; Guan, Y.; Zhou, K.; Kou, Y.; Zhou, X.; Zhang, Q. Spatiotemporal analysis of the interactions between ecosystem services in arid areas and their responses to urbanization and various driving factors. *Remote Sens* **2024**, *16*, 520. [CrossRef]
48. Czarnecki, A.; Milczarek-Andrzejewska, D.; Widła-Domaradzki, Ł.; Jórasz-Żak, A. Conflict dynamics over farmland use in the multifunctional countryside. *Land Use Policy* **2023**, *128*, 106587. [CrossRef]
49. Zhao, X.; Feng, T.; Pengtao, Z.; Boyang, H.; Lei, X. Dynamic simulation and characteristic analysis of county production-living-ecological spatial conflicts based on CLUE-S model. *Acta Ecol. Sin.* **2019**, *39*, 5897–5908. [CrossRef]
50. Chen, L.T.; Zhang, A.L.; Wen, L.J. Complex interactions of ecosystem services and their dynamic changes in response to land-use conflicts—A network analysis in the Yangtze River Economic Belt, China. *Land Use Policy* **2025**, *155*, 107582. [CrossRef]
51. Lawrence, M.; Homer-Dixon, T.; Janzwood, S.; Rockstom, J.; Renn, O.; Donges, J.F. Global polycrisis: The causal mechanisms of crisis entanglement. *Glob. Sustain.* **2024**, *7*, e6. [CrossRef]
52. Matlovič, R.; Matlovičová, K. Polycrisis in the Anthropocene as a key research agenda for geography: Ontological delineation and the shift to a post disciplinary approach. *Folia Geogr.* **2024**, *66*, 5–33. Available online: https://www.foliageographica.sk/unipo/journals/2024-66-1/700/ (accessed on 16 March 2026).
53. Sun, L.; Yu, H.; Sun, M.; Wang, Y. Coupled impacts of climate and land use changes on regional ecosystem services. *J. Environ. Manag.* **2023**, *326*, 116753. [CrossRef]

Disclaimer/Publisher's Note: The statements, opinions and data contained in all publications are solely those of the individual author(s) and contributor(s) and not of MDPI and/or the editor(s). MDPI and/or the editor(s) disclaim responsibility for any injury to people or property resulting from any ideas, methods, instructions or products referred to in the content.